Modular Response in Free Quantum Fields: A KMS/FDT Theorem and Conditional Extensions

[clg][1]

[1] *[Institutions]*

(Dated:)

Part I (Theoremic core, free/Gaussian Hadamard QFT). We prove that, for small causal diamonds (CHM) in locally Hadamard states and within a safe window $\epsilon_{\rm UV} \ll \ell \ll \min\{L_{\rm curv}, \lambda_{\rm mfp}, m_i^{-1}\}$, the MI/moment-kill projector isolates a finite ℓ^4 modular response with coefficient equal to its flat-space value; the projected KMS/FDT susceptibility is positive; and coarse-graining over the wedge family produces the universal weak-field prefactor $5/12 = (4/3) \times (5/16)$. The fractional KMS defect between CHM diamonds and half-spaces scales as $\mathcal{O}((\ell/L_{\rm curv})^2) + \mathcal{O}((\ell H)^2)$. The QFT sensitivity is $\beta = 2\pi C_T I_{00} = 0.02086 \pm 0.00105$ (conservative 5% shared systematics). A scheme-invariant background relation *suggests* $\Omega_\Lambda = \beta\, f\, c_{\rm geo}$ *conditional* on our coarse-graining and analyticity assumptions.

Part II (Conditional extensions). We separate *definition* (flat-space ε from modular response) from *mapping*. Rather than impose the standard EFT-of-DE α-basis, we adopt a quasi-static closure that keeps operational distances GR-like (no additional lensing coupling $\Sigma \simeq 1$) while modifying growth via $\mu(\varepsilon, s) = 1/(1+\frac{5}{12}\varepsilon\, s(x))$ with $s(x)$ a local, covariant environment modulation derived from the action. KMS/FDT positivity motivates an entropy-driven law $d\varepsilon/d\ln a \geq 0$ with a *conditional* background budget $\int \varepsilon\, d\ln a = \Omega_\Lambda$. We then prove a *No-Go Lemma* showing any linear kernel fails to yield Tully–Fisher scaling and introduce a *quasistatic elastic sector* (AQUAL form, derived as the SK static limit) with the *same* fixed acceleration $a_0 = \frac{5}{12}\Omega_\Lambda^2 c H_0$. The elastic sector is convex, well-posed, obeys Solar–System curvature gating, produces $\Phi = \Psi$ at working order (no slip), and leaves linear cosmology intact via a causal SK filter.

Part III (Exploratory). (i) An *optional*, shock-selective *optical* channel (D′) reduces Σ only in high-shear shocked gas to address Bullet-type lensing offsets while preserving FRW distances, with a principled SK/BRSSS derivation path connecting the amplitude to ICM transport coefficients. (ii) A compact thermodynamic interpretation of the projected modular response: a Clausius-like identity holds at working order in the MI/moment-kill channel, and the FRW budget may be viewed as a *coarse-grained* Clausius normalization *conditional* on our KMS→FRW hypotheses. (iii) *Linkage to global entropic gravity (Bianconi 2025)* via small-diamond MI matching and observational discriminants.

Referee-guided additions. We (A) formalize an MI-smeared null-energy positivity (free fields; projected QEI), (B) make explicit the RG/operator-spectrum bridge pinning β to C_T and clarifying anomaly channels, (C) expose SM bookkeeping tied to the safe-window fraction f_V and curvature gating $s(\chi_g)$ so that GR dominance is recovered wherever heavy sectors or strong curvature suppress the MI channel, and (D) add the *No-Go Lemma + elastic SK/AQUAL sector* with fixed a_0, no slip, Solar–System compliance, and cosmology/galaxy separation.

READER'S MAP: PART I (THEOREM) VS. PART II (CONDITIONAL) VS. PART III (EXPLORATORY)

Part I (Secs. I–V, IV, XIA–B; Apps. XXI–XXV): proven results for free/Gaussian Hadamard fields at working order, SM bookkeeping, and first-principles positivity/RG clarifications.
Part II (Secs. VI–VIII, IX, XXXII, XIC; Apps. XXVI–XXVII, XXVIII): conditional mapping for growth ($\mu(\varepsilon, s)$), *Linear No-Go* (Sec. VII), and *Elastic quasistatic sector* (Sec. VIII) with Solar–System gating, no slip, and BTFR; causal SK separation of regimes.
Part III (Secs. XIII, XX, XVII; Apps. XXX, XXXI): exploratory shock-selective optics (D′); thermodynamic interpretation; and linkage to Bianconi's global entropic gravity.

I. SCOPE, WORKING ORDER, AND SAFE-WINDOW QUANTIFICATION (PART I)

a. Working order and state class. We work to $\mathcal{O}(\ell^4)$ in the MI/moment-kill projector channel, treating curvature/contact terms as $\mathcal{O}(\ell^6)$. States are locally Hadamard.

b. KMS applicability (CHM diamonds). Exact BW KMS holds for half-spaces; CHM diamonds inherit it with fractional defect $\mathcal{O}((\ell/L_{\rm curv})^2) + \mathcal{O}((\ell H)^2)$ (App. XXV).

c. Safe-window volume fraction. Define a conservative admissible scale

$$\ell_{\max}(x) \equiv \zeta \, \min\left\{L_{\rm curv}(x),\ \lambda_{\rm mfp}(x),\ m_i^{-1}(x)\right\}, \qquad \zeta = 0.1. \tag{1}$$

Using Press–Schechter/Sheth–Tormen mass functions and NFW curvature proxies $L_{\rm curv}^{-2} \sim (R_{abcd}R^{abcd})^{1/2}$ with substructure excision parameter ξ, we estimate the comoving volume fraction $f_V(\ell_{\min}) = {\rm Vol}\{x : \ell_{\max}(x) > \ell_{\min}\}/{\rm Vol}_{\rm tot}$. A semi-analytic survey (App. XXVI) shows voids dominate f_V, while dense cores lack a window; representative values at $z\sim 0$ for $\ell_{\min} \in [1, 100]$ pc are $f_V \sim 0.6–0.95$ for $\xi \in [0.2, 0.5]$. This enters only as a domain-of-validity indicator.

d. Spectrum caveat. The admissible window $\epsilon_{\rm UV} \ll \ell \ll \min\{L_{\rm curv}, \lambda_{\rm mfp}, m_i^{-1}\}$ is understood to apply to sectors that contribute at working order. Massive sectors with $\ell \gg m_i^{-1}$ are exponentially suppressed and, after MI/moment–kill subtraction, do not re-introduce lower moments or $\ell^4 \log \ell$ terms. Thus the ℓ^4 coefficient is dominated by massless/light fields while heavy fields decouple in this channel. *See Sec. IV for SM bookkeeping that packages light-field multiplicity into a single $\varepsilon_{\rm SM}$.*

e. Angle invariance as a null test. The continuous-angle product $\mathcal{C}_\Omega = f(\theta)\, c_{\rm geo}(\theta)$ is analytic and θ-independent; residuals are shown as a null check, not a precision claim.

II. A2–KMS THEOREM (GAUSSIAN/HADAMARD SECTOR)

Theorem 1 (Projected modular response and positivity)**.** *Let $\mathcal{Q}$ be a free (Gaussian) QFT on a globally hyperbolic spacetime and ρ a locally Hadamard state. For a causal diamond of radius ℓ with $\ell \ll L_{\rm curv}$ and the MI/moment-kill projector that cancels r^0 and r^2 moments, the MI-subtracted modular response obeys*

$$\delta\langle K_{\rm sub}\rangle = (2\pi C_T I_{00})\, \ell^4\, \delta\varepsilon + \mathcal{O}(\ell^6), \tag{2}$$

with coefficient equal to the flat-space value. The retarded susceptibility χ_{QK} in the projected channel is positive (FDT), and wedge averaging yields the universal weak-field prefactor $5/12$. The fractional deviation from BW KMS is $\mathcal{O}((\ell/L_{\rm curv})^2) + \mathcal{O}((\ell H)^2)$.

Corollary 1 (Conditional background statement)**.** *Under the coarse-graining and analyticity assumptions of Sec. X, the FRW zero mode* suggests *the scheme-invariant relation $\Omega_\Lambda = \beta\, f\, c_{\rm geo}$ with $\beta = 2\pi C_T I_{00}$. We treat this as a conditional statement rather than a theorem.*

III. QFT INPUT: $\beta = 2\pi C_T I_{00}$ AND ERROR BUDGET

We evaluate β via four independent routes: (a) real-space CHM; (b) spectral/Bessel; (c) Euclidean time-slicing; (d) replica finite-difference. The spread is $\lesssim 1\%$. We adopt a conservative

$$\beta = 0.02086 \pm 0.00105 \quad (5\% \text{ shared systematics}). \tag{3}$$

Angle invariance is used as a null residual test.
Here C_T denotes the flat-space stress-tensor two-point normalization, e.g. $\langle T_{ab}(x)\, T_{cd}(0)\rangle = C_T\, \mathcal{I}_{abcd}(x)/|x|^{2d}$ in d dimensions (see Osborn–Petkou).
Benchmark (convention). For a free, massless real scalar in $d = 4$ and our normalization, $C_T = 1/(120\pi^2)$, which yields $\beta \simeq 0.02086$ via Eq. (4).
Implementation consistency (note). The normative constants used for the numerical reproductions are

$$C_T = \frac{1}{120\pi^2}, \qquad (\sigma_1, \sigma_2) = \left(\tfrac{1}{2}, 2\right), \qquad (a, b) = \left(\tfrac{4}{5}, \tfrac{1}{5}\right),$$

with the moment-kill identities enforced exactly (App. XXI). Helper scripts (`beta_methods_v2.py`, `referee_pipeline.py`) print these values alongside the computed I_{00} to prevent normalization drift.[1]
Reproducibility (non-circular). We use a two–scale MI/moment-kill subtraction with a top-hat window on 3-balls

$$W_\ell(r) = \frac{3}{4\pi\ell^3}\,\Theta(\ell - r), \qquad \mathcal{W}_\ell := \int_{B_\ell} W_\ell - \ a\int_{B_{\sigma_1\ell}} W_{\sigma_1\ell} - \ b\int_{B_{\sigma_2\ell}} W_{\sigma_2\ell}.$$

---

[1] In earlier development branches some convenience flags defaulted to alternate normalizations (e.g. $C_T = 3/\pi^4$) and near-unity MI scales. These have been disabled in the archival runners; the paper's conventions are authoritative.

The two moment-kill conditions (cancelling r^0 and r^2 for any smooth radial F) fix

$$a+b=1, \qquad a\,\sigma_1^2+b\,\sigma_2^2=1 \implies a=\frac{\sigma_2^2-1}{\sigma_2^2-\sigma_1^2}, \quad b=\frac{1-\sigma_1^2}{\sigma_2^2-\sigma_1^2}.$$

In our runs we take

$$(\sigma_1,\sigma_2)=\left(\tfrac{1}{2},\,2\right), \qquad (a,b)=\left(\tfrac{4}{5},\,\tfrac{1}{5}\right)=(0.8,0.2).$$

With these weights the projected ℓ^4 coefficient evaluates to

$$I_{00}=3.932017 \ \ \text{(dimensionless)},$$

so with $C_T=1/(120\pi^2)$ one obtains $\beta=2\pi C_T I_{00}=0.02086$ as quoted. The helper script `beta_methods_v2.py` echoes both $(a,b;\sigma_1,\sigma_2)$ and the numeric I_{00}.

IV. STANDARD-MODEL SECTOR: BOOKKEEPING AND DECOUPLING AT WORKING ORDER

a. What is being linked. At working order the MI/moment–kill channel defines the dimensionless state variable $\varepsilon(x)$ through

$$\delta\langle K_{\rm sub}\rangle=\beta\,\ell^4\,\delta\varepsilon+\mathcal{O}(\ell^6) \quad \text{[Eq. (4)]}.$$

This subsection clarifies how the *Standard–Model (SM)* content enters ε and why heavy states decouple.

b. Species sum and decoupling. Write ε as a weighted sum over species i:

$$\varepsilon(x)=\sum_i w_i\,\varepsilon_i(x), \qquad w_i \text{ counts effective dof (helicity/polarization, internal factors).}$$

In a diamond of size ℓ, fields with $m_i\ell\gg 1$ are exponentially suppressed in the projected channel; after the MI/moment–kill subtraction they do *not* re-introduce lower moments nor $\ell^4\log\ell$ terms. Parametrically,

$$\varepsilon_i(x)\ \propto\ e^{-m_i\ell} \quad \text{for } m_i\ell\gg 1,$$

so the ℓ^4 coefficient is dominated by massless/light fields while heavy fields decouple.

c. Packaging the light SM content. It is convenient to define a single light-sector variable

$$\varepsilon_{\rm SM}(x)\equiv\sum_{i\in\text{light}} c_i\,\varepsilon_i(x),$$

where c_i packages the relevant multiplicities (helicity/polarization, internal quantum numbers) of each light SM species under the MI projection. All subsequent working-order formulas may then be read with $\varepsilon\to\varepsilon_{\rm SM}$ when SM content is explicitly considered.

d. Coupling to gravity at working order. The only background scalar that survives the MI/moment–kill projection and modifies weak-field growth while keeping distances GR-like is the Planck-mass renormalization $\delta\ln M^2=\beta\,\delta\varepsilon$ (Assumption D). Multiplicities therefore simply rescale ε (hence μ); they do *not* change β or the universal weak-field bookkeeping that fixes the 5/12 prefactor:

$$\mu(\varepsilon,s)=\frac{1}{1+\frac{5}{12}\,\varepsilon\,s(x)} \quad\longrightarrow\quad \mu(\varepsilon_{\rm SM},s)=\frac{1}{1+\frac{5}{12}\,\varepsilon_{\rm SM}\,s(x)}.$$

e. Environment and distances. The environment scalar $s(x)$ is geometric (built from curvature invariants) and independent of particle content at this order; FRW distances remain GR-like ($\Sigma\simeq 1, c_T=1$). The observed lensing amplitude changes only indirectly through altered growth.

f. Practical note and f_V linkage. In cosmological applications one sets a light-sector threshold $m_i\ell\lesssim 1$ (with ℓ within the safe window) and computes $\varepsilon_{\rm SM}$ using the appropriate c_i. As the environment varies, *field regimes can re-enter* $\varepsilon_{\rm SM}$ smoothly. Dense regions with no safe window contribute negligibly to the MI channel; voids dominate the valid domain via f_V (App. XXVI). GR dominance is ensured either by strong curvature ($s(\chi_g)\to 0$) or by heavy-sector decoupling ($m_i\ell\gg 1$).

V. WEAK-FIELD PREFACTOR 5/12

The isotropic BW channel gives $\langle T_{kk}\rangle = (1+w)\rho$ with UV $w = 1/3 \Rightarrow 4/3$. Averaging over CHM segments yields $5/16$, so $5/12 = (4/3)\times(5/16)$. Details in Sec. V.

VI. DEFINITION VS. MAPPING (PART II; CONDITIONAL)

a. Definition (flat-space QFT).

$$\delta\langle K_{\rm sub}(\ell)\rangle = \underbrace{(2\pi C_T I_{00})}_{\beta}\,\ell^4\,\delta\varepsilon(x) + \mathcal{O}(\ell^6). \tag{4}$$

b. Mapping (constitutive; beyond the α-basis). We *do not* impose the linear EFT-of-DE α-parameter mapping at working order. Instead, we adopt a quasi-static closure that keeps operational distances GR-like while modifying growth:

$$\nabla^2\Phi \;=\; 4\pi G a^2\rho_m\,\mu(\varepsilon,s), \qquad \mu(\varepsilon,s) = \frac{1}{1+\frac{5}{12}\varepsilon\,s(x)}, \tag{5a}$$

$$\nabla^2\frac{\Phi+\Psi}{2} \;=\; 4\pi G a^2\rho_m, \qquad (\Sigma\simeq 1 \text{ on FRW and in laminar flows}). \tag{5b}$$

Here $s(x)$ is a local scalar built from curvature (Sec. XV); in FRW, Weyl $=0 \Rightarrow \chi_g = 0 \Rightarrow s = 1$. *Beyond working order we make no stability claims absent an action; $\mu(\varepsilon,s)$ serves as a falsifiable diagnostic with* $\Sigma \simeq 1$. Matter obeys the standard continuity and Euler equations. This closure preserves the Bianchi identity at working order because $s(x)$ is a scalar; an action-level realization and frame-independence are given below (Remark VI A). *Optional Assumption D' (Sec. XIII)* introduces a *shock-selective* lensing modification $\Sigma(x) < 1$ localized to high-shear gas while keeping FRW $\Sigma \simeq 1$.
Remark on lensing amplitude. $\Sigma \simeq 1$ denotes no additional lensing coupling in the baseline; the observed lensing signal still changes through the altered growth $D(a)$. Under Assumption D$'$, Σ may be reduced *locally* in shocked gas ($\mathcal{S}_{\rm shock} \gg 1$) without affecting FRW.

c. EFT stub (derivation of 5/12). At quasi-static, sub-horizon scales, a background variation $\delta\ln M^2 = \beta\,\delta\varepsilon$ rescales the Poisson coupling as $G \to G_{\rm eff} = G/(1+\Delta)$ with Δ fixed by the universal weak-field bookkeeping. In the isotropic BW channel the contraction 4/3 and the segment ratio 5/16 (Sec. V) give $\Delta = \frac{5}{12}\varepsilon$, hence

$$\mu(\varepsilon,s) = \frac{G_{\rm eff}}{G} = \frac{1}{1+\frac{5}{12}\varepsilon\,s(x)}, \tag{6}$$

consistent with Eqs. (5).

d. Trial action (outlook). A possible action-level route consistent with our closure is to consider an effective term that modulates M^2 via the modular response,

$$S_{\rm trial} = \int d^4x\,\sqrt{-g}\left[\frac{M^2}{2}R + \lambda\,(\delta\ln M^2)\,\mathcal{K}[g;\ell] + \cdots\right],$$

where $\mathcal{K}$ is a local covariant scalar capturing the projected channel at working order and λ a running coefficient. While only illustrative, this shows how $\delta\ln M^2 = \beta\,\delta\varepsilon$ could arise from an action (cf. [6, 8]).

A. Frame-independence of throttling (remark)

Throttling here means the reduction of the effective gravitational coupling relative to GR caused by the background state variable $\varepsilon(a)$ and a local environment factor $s(x)$ that encodes curvature/inhomogeneity. In the Jordan frame we take

$$M_*^2(x,a) = M^2\left[1+\tfrac{5}{12}\,\varepsilon(a)\,s(x)\right], \qquad s(x) = \frac{1}{1+(\chi_g/\chi_\star)^q} + \mathcal{O}\Big(\frac{R}{m_s^2}\Big),$$

so the quasi-static Poisson law reads

$$\nabla^2\Phi \simeq \frac{4\pi G a^2 \rho_m\, \delta}{1+\frac{5}{12}\,\varepsilon(a)\,s(x)} \quad \Rightarrow \quad G_{\rm eff}(x,a) = \frac{G}{1+\frac{5}{12}\,\varepsilon(a)\,s(x)}.$$

Thus throttling is present everywhere, while its magnitude is amplitude–modulated by the local invariant $\chi_g = \ell^2\sqrt{C_{abcd}C^{abcd}}$: in weak fields ($\chi_g \ll \chi_\star$) one has $s \to 1$ and the full background rescaling $G_{\rm eff} = G/(1+\frac{5}{12}\varepsilon)$; in strong fields ($\chi_g \gg \chi_\star$) one has $s \to 0$ and $G_{\rm eff} \to G$ (Solar–System compliance).

A conformal map to the Einstein frame,

$$\tilde g_{\mu\nu} = \Omega^2 g_{\mu\nu}, \qquad \Omega^2 = 1+\tfrac{5}{12}\,\varepsilon(a)\,s(x),$$

renders M_* constant and shifts the same throttling into the matter coupling. To working order in our MI/moment-kill channel, gradients of Ω and of χ_g enter only at $\mathcal{O}\big((\ell/L_{\rm curv})^2\big)$ and $\mathcal{O}(R/m_s^2)$, consistent with the error budget in Eq. (9) and App. XXV; the observables of interest are frame–independent at this order: growth is governed by

$$\mu(\varepsilon,s) = \frac{1}{1+\frac{5}{12}\,\varepsilon(a)\,s(x)},$$

and distances remain GR-like ($\Sigma \simeq 1$, $c_T = 1$).[2]

Scale-separation note. The *local* modular response enters gravity solely as a renormalization $\delta \ln M_*^2 = \beta\,\delta\varepsilon$ of the Planck mass; the Einstein equations then propagate this renormalization to cosmological scales through the standard gravitational coupling. No macroscopic quantum coherence or ad hoc coarse-graining is required, and the Jordan↔Einstein map above makes this statement frame-independent at working order.

A simple way to realize $s(x)$ is as an auxiliary heavy scalar that minimizes a local potential

$$\mathcal{V}(s;\chi_g) = \frac{M^2 m_s^2}{2}\left[s - \frac{1}{1+(\chi_g/\chi_\star)^q}\right]^2,$$

so that the algebraic EOM enforces $s = [1+(\chi_g/\chi_\star)^q]^{-1} + \mathcal{O}(R/m_s^2)$. Choosing $m_s^2 \gg H_0^2$ ensures adiabatic tracking.

Constraints (working order). (i) Choose $m_s^2 \gg H_0^2$ so $s(x)$ adiabatically tracks $[1+(\chi_g/\chi_\star)^q]^{-1}$ and the $\mathcal{O}(R/m_s^2)$ offset is negligible. (ii) The Planck-mass drift $\alpha_M = d\ln M_*^2/d\ln a = \frac{(5/12)\,s\,d\varepsilon/d\ln a}{1+(5/12)\varepsilon s}$ is naturally small under our monotone $\varepsilon(a)$. (iii) In FRW, Weyl $= 0$ so curvature-weighted corrections vanish; in LSS they are $\mathcal{O}\big((\ell/L_{\rm curv})^2\big)$.

Weak-field acceleration (toy/conditional; clarification). Because $s \to 1$ in low curvature, the weak-field normalization implies a MOND-like scale

$$a_0 = \frac{5}{12}\,\Omega_\Lambda^2\, c\, H_0, \tag{7}$$

Using the baseline $\Omega_\Lambda = 0.685$ and $H_0 = 70.9$ km s^{-1} Mpc^{-1}, this gives $a_0^{\rm eff} \approx 1.2\times10^{-10}$ m s^{-2} in the weak-field limit ($s \simeq 1$); and the effective $a_0^{\rm eff}$ is *enhanced* in weak-field regimes by the *derived* $s \to 1$ (not imposed), while Solar–System compliance follows from $s(\chi_\odot) \ll 1$ (Sec. XV). Pipeline values propagate the ±5% uncertainty in β.

VII. LINEAR-KERNEL NO-GO FOR TULLY–FISHER

Lemma 1 (Linear-kernel no-go)**.** *Let Φ be determined from ρ by a translation/rotation-invariant* linear *map with tempered kernel G:*

$$\Phi(\mathbf{x}) = (G*\rho)(\mathbf{x}), \qquad G(\mathbf{x}) = \frac{1}{(2\pi)^3}\int \frac{\tilde g(\mathbf{k})}{k^2}\, e^{i\mathbf{k}\cdot\mathbf{x}}\, d^3k, \quad \tilde g(\mathbf{k}) > 0,$$

and assume that outside a bounded mass distribution the stationary field equation reduces to a linear constant-coefficient elliptic operator. Then the exterior field decays as $\Phi \sim -\mathcal{G}_{\rm eff}M/r$, so $g = |\nabla\Phi| = \mathcal{G}_{\rm eff}GM/r^2 + o(r^{-2})$ and $v_\infty^4 \propto M^2$. Thus a linear kernel cannot *yield the Tully–Fisher scaling $v_\infty^4 \propto M$.*

Sketch. In vacuum the solution is harmonic (up to renormalization $\mathcal{G}_{\rm eff}$); Liouville/Rellich imply the only decaying solution is $1/r$, hence $g \propto r^{-2}$. Any linear, isotropic nonlocality rescales $\mathcal{G}_{\rm eff}$ but preserves the $1/r^2$ falloff.

---

[2] This remark complements Assumption D (Sec. XII B): the working-order modification resides in a state- and environment-dependent M_*^2 with no additional lensing coupling. A failure would manifest as our falsifiers in Sec. XIX, e.g. a significant GW/EM distance split or a persistent $\ell^4 \log \ell$ term.

VIII. ELASTIC QUASISTATIC SECTOR (AQUAL FROM SK STATIC LIMIT)

a. Static elastic action and field equation. In the quasistatic limit of the Schwinger–Keldysh (in–in) effective action, a causal retarded kernel $\mathcal{K}^{\rm el}$ reduces to a local, convex functional for the Newtonian potential Φ:

$$\boxed{\mathcal{L}_{\rm el}(\Phi,\nabla\Phi) \;=\; \frac{a_0^2}{8\pi G}\,F(Y) \;-\; \rho\,\Phi, \quad Y\equiv\frac{|\nabla\Phi|^2}{a_0^2}}$$

with $F\in C^2([0,\infty))$, $F'(Y)=\mu(Y)>0$, $F''(Y)\geq 0$, and asymptotics

$$\mu(Y)\xrightarrow{Y\gg1}1, \qquad \mu(Y)\xrightarrow{Y\ll1}\sqrt{Y}.$$

Variation yields the AQUAL field equation [22]:

$$\nabla\cdot\big(\mu(Y)\,\nabla\Phi\big)=4\pi G\,\rho. \tag{8}$$

b. Deep regime and BTFR (galaxies). For spherical mass M, in the deep regime ($g\ll a_0\Rightarrow\mu\simeq\sqrt{Y}=g/a_0$) one obtains

$$\frac{g}{a_0}\,g=\frac{GM}{r^2} \quad\Rightarrow\quad g(r)=\frac{\sqrt{GMa_0}}{r}, \qquad v_\infty^4=GMa_0.$$

Thus the baryonic Tully–Fisher relation follows directly.

c. Uniform ellipticity / well-posedness. The linearization tensor

$$\mathcal{A}_{ij}(\nabla\Phi)=\mu\,\delta_{ij}+\frac{2\mu'}{a_0^2}\,\partial_i\Phi\,\partial_j\Phi$$

is uniformly elliptic provided $\mu>0$ and $\mu+2Y\mu'(Y)>0$, which holds for the convex class above. Existence/uniqueness follows from standard elliptic theory.

d. Minimal convex interpolant (derivation).

Proposition 1 (Minimal Stieltjes elastic law)**.** *Under the constraints: (i) locality and isotropy in the quasistatic SK limit, (ii) convexity/ellipticity, (iii) single scale a_0, and (iv) the asymptotic limits $\mu(x)\sim x$ as $x\to0$ and $\mu(x)=1-1/x+O(1/x^2)$ as $x\to\infty$, the unique minimal Padé/Stieltjes interpolant is*

$$\boxed{\mu(x)=\frac{x}{1+x}} \quad\Longleftrightarrow\quad \boxed{\mu(Y)=\frac{\sqrt{Y}}{1+\sqrt{Y}}}.$$

This law is convex ($F''\geq0$), uniformly elliptic ($\mu+2Y\mu'(Y)>0$), and introduces no extra scales beyond a_0. The corresponding convex potential is

$$F(Y)=Y-2\sqrt{Y}+2\ln(1+\sqrt{Y}).$$

Alternative convex families (e.g. $\mu_n(x)=x/(1+x^n)^{1/n}$) exist but differ only in the transition regime; the minimal Padé law is the unique choice fixed by the above constraints.

e. Same fixed acceleration scale. We identify

$$\boxed{a_0=\frac{5}{12}\,\Omega_\Lambda^2\,c\,H_0}$$

from the capacity (Part I/II) channel; thus the BTFR normalization is **fixed** (no fit).

f. Solar–System compliance (curvature gate). Insert the same curvature gate via $a_0\to a_0^{\rm eff}(x)=a_0\,s(\chi_g)^p$ (with $p\geq1$ integer). Using Sec. XV one has $s(\chi_\odot)\lesssim10^{-5}$, hence $a_0^{\rm eff}\ll10^{-15}\,a_0$ in the Solar System, fully suppressing elastic effects.

g. Lensing equals dynamics (no slip). Place the static elastic density in the quasistatic Einstein system symmetrically so that $\Phi=\Psi$ at working order; equivalently, couple the AQUAL density to $(\Phi+\Psi)/2$. Then the lensing potential 2Φ tracks the same μ that governs dynamics, and galaxy–galaxy lensing matches rotation-curve inferences.

IX. CAUSAL SK SEPARATION OF COSMOLOGY VS. GALAXIES

In the full SK theory, the elastic kernel depends on frequency and wavenumber, $\mathcal{K}^{\rm el}(\omega,k)$. Causality and finite relaxation imply a factor

$$\mathcal{K}^{\rm el}(\omega,k)=\mathcal{Q}(\omega,k)\,\mathcal{K}^{\rm el}(0,k),\qquad \mathcal{Q}(0,k)=1,\quad |\mathcal{Q}(\omega\sim H,k\lesssim k_{\rm LSS})|\ll 1.$$

Thus:

- **Linear cosmology (FRW, LSS):** $\omega\sim H$, $k\lesssim k_{\rm LSS}\Rightarrow\mathcal{Q}\approx 0$. Dynamics is governed by the *capacity channel* ($\mu(\varepsilon,s)<1$), preserving distances and the S_8 suppression.
- **Quasistatic galaxies:** $\omega\to 0$, $k\gtrsim k_{\rm gal}\Rightarrow\mathcal{Q}\to 1$. The *elastic* AQUAL sector governs dynamics and lensing with fixed a_0.

No new dimensional scales are introduced; $\mathcal{Q}$ encodes scale separation already present in the SK influence functional.

X. COVARIANT KMS → FRW LINK AND ERROR CONTROL

Let s denote modular time with $\beta_{\rm KMS}=2\pi/\kappa$ locally, where κ is the local boost surface gravity so that the approximate conformal Killing field ξ^a satisfies $\xi^a\nabla_a=\kappa\,\partial_s$. Averaging the retarded kernel over a comoving congruence of diamonds and reparametrizing $s\mapsto\ln a$ induces the FRW background factor $f\,c_{\rm geo}$; diffeomorphism covariance is preserved because the averaging functional depends only on local curvature scalars and the diamond foliation. The total fractional defect in the kernel obeys

$$\frac{\delta\chi}{\chi_{\rm BW}}=\mathcal{O}\Big((\ell/L_{\rm curv})^2\Big)+\mathcal{O}\big((\ell H)^2\big)\quad\approx\quad 10^{-12}+10^{-18}\tag{9}$$

for $\ell\sim 10\,{\rm pc}$, $L_{\rm curv}\sim 10\,{\rm Mpc}$, $H^{-1}\sim 4\,{\rm Gpc}$.

Proposition 2 (FRW budget identity (conditional; analyticity hypothesis))**.** *Assume: (H1) locality and rapid decay of the spatially averaged, projected retarded kernel so that its reparametrization defines a distribution in* $\ln a$*; (H2) adiabatic evolution through matter domination so that* $J(a)=ds/d\ln a\propto H(a)^{-1}$ *varies slowly; (H3) preservation of KMS analyticity of the averaged kernel under the reparametrization* $s\to\ln a$*; and (H4) negligible CHM vs. half-space deviation at working order (App. XXV). Then*

$$\Big\langle\int\chi^{\rm proj}_{QK}(a,a')\,d^3x\Big\rangle=\beta\,f\,c_{\rm geo}\,\delta(\ln a-\ln a')+\dots$$

and integrating the entropy-driven evolution $d\varepsilon/d\ln a=\sigma(a)I(a)\ge 0$ *yields the coarse-grained identity*

$$\int_{a_i}^{1}\varepsilon(a)\,d\ln a\;=\;\Omega_\Lambda\;=\;\beta\,f\,c_{\rm geo},\tag{10}$$

used as a normalization under (H1)–(H4).

Operational diagnostic. The routine `referee_pipeline.py` reports a scalar residual $R_{\rm nonloc}\equiv\sum_{i\neq 0}\big|\bar\chi^{\rm proj}(\Delta_i)\big|\,\Delta(\ln a)_i$ outside the contact bin; by default we take the central bin(s) with $|\Delta(\ln a)|\le\Delta_0$ as "contact". Declare failure if $R_{\rm nonloc}/\sigma_{\rm boot}>3$ *and* the contact weight $w_0<0.95$.

a. Rigor note. A full microlocal proof of (H3)—preservation of KMS analyticity under the coarse-grained reparametrization $s\to\ln a$—is deferred to future work in the spirit of Hollands–Wald [10].

b. Thermodynamic analogy (pointer). The entanglement first law suggests a Clausius-like analogy (Sec. XX), *conditional* on (H1)–(H4), with MI projection avoiding CGM's marginality issues (App. XXVII).

XI. REFEREE-GUIDED FIRST-PRINCIPLES CLOSURES AND TESTS

A. MI-smeared null-energy bound (projected; proven for free fields)

Statement (free/Gaussian sector). Let k^a be a null generator of the CHM diamond and $h_\ell(x)\ge 0$ a smooth, compactly supported sampling function adapted to the MI window (normalized to unit weight). Define the MI-smeared null contraction

$$\mathcal{E}^{\rm MI}_\ell\;\equiv\;\int d^4x\,d^4x'\,h_\ell(x)\,h_\ell(x')\,\langle T_{ab}(x)k^ak^b\rangle^{\rm proj}_{\rm sub}\,.$$

Then, in free Hadamard theories,

$$\mathcal{E}_\ell^{\rm MI} = \underbrace{\langle \delta K_{\rm sub}, \delta K_{\rm sub} \rangle_{\rm BKM}}_{\geq 0} \times \mathcal{N}_\ell \quad \Rightarrow \quad \mathcal{E}_\ell^{\rm MI} \geq 0$$

with a calculable ℓ-dependent normalization $\mathcal{N}_\ell > 0$ fixed by the MI projector.

Consequence. The MI/moment-kill subtraction yields a *QEI-like* positive quadratic form for null energy in the projected channel (free fields: exact; interacting: Assumption C).

B. RG/operator-spectrum bridge and anomaly guardrails

Bridge. β is tied to the stress-tensor two-point normalization C_T; our ℓ^4 universality relies on the MI projector removing $\Delta < 4$ contributions. Protected marginal operators would show up as $\ell^4 \log \ell$ in this channel; the *absence* of such a term (checked numerically) is therefore a guardrail (Sec. XIX, (i)).
Anomalies. Parity-odd and trace-anomaly structures do not contribute at $\mathcal{O}(\ell^4)$ in the MI-projected, parity-even channel; they either vanish by symmetry or are curvature-suppressed by $\mathcal{O}((\ell/L_{\rm curv})^2)$.

C. Where GR dominates: f_V & curvature gating (SM-aware)

Dense, high-curvature regions either (i) lack a safe window (small f_V locally) or (ii) trigger $s(\chi_g) \to 0$ so that $G_{\rm eff} \to G$. Heavy SM sectors drop out when $m_i \ell \gg 1$. Thus GR dominance is guaranteed wherever MI control fails or curvature is large, while voids (dominant in f_V) carry the clean MI signal.

XII. ASSUMPTIONS FOR INTERACTING EXTENSIONS AT WORKING ORDER (PART II; STATED AND TEST CRITERIA)

A. Assumption C (stated; test criteria): Relative entropy $\leftrightarrow$ canonical energy in the projected diamond

Statement. For a local algebra $\mathcal{A}(B_\ell)$ of an interacting Hadamard QFT obeying the microlocal spectrum condition and time-slice axiom, the MI/moment-kill projected second variation of Araki relative entropy equals the canonical-energy quadratic form of the projected stress tensor, up to $\mathcal{O}(\ell^6)$ remainders, with a positive-definite projected kernel $\chi_{QK}^{\rm proj}$.

Rationale (sketch). (i) The second variation is the Bogoliubov–Kubo–Mori metric. (ii) The MI/moment-kill projector cancels local counterterms to $\mathcal{O}(\ell^4)$ (App. XXI), conjectured to persist in interacting Hadamard QFTs (App. XXVII). (iii) Diffeomorphism Ward identities match the BKM quadratic form to canonical energy in the CHM channel. (iv) Positivity follows from KMS/BKM positivity in the projected channel.

a. Operational tests (pass/fail).

- **Positivity test (substrates):** The projected, integrated retarded kernel $\int \chi_{QK}^{\rm proj}\, d^4x\, d^4x'$ is nonnegative in Gaussian chains (exact) and HQTFIM (numerical tolerance).
- **No-$\ell^4 \log \ell$ falsifier:** The MI/moment-kill channel exhibits no $\ell^4 \log \ell$ term.
- **Plateau stability:** Varying MI windows leaves the residual plateau $\sim \mathcal{O}(\ell^6)$.

B. Assumption D (stated; test criteria): Uniqueness of the M^2 coupling at working order

Statement. In the $c_T = 1$, $\alpha_B = 0$ EFT corner linearized about FRW, with isotropy, parity, and time-reversal, the only background scalar coupling that survives the MI/moment-kill projection at $\mathcal{O}(\ell^4)$ and modifies the weak-field growth sector while keeping distances GR-like is $\delta \ln M^2$; other diffeomorphism-invariant local scalars are projected out, forbidden by sector constraints, or curvature-suppressed by $\mathcal{O}((\ell/L_{\rm curv})^2)$.

a. Operational tests (pass/fail).

- **GR-like distances:** $|d_L^{\rm GW}/d_L^{\rm EM} - 1| \lesssim 5 \times 10^{-3}$.
- **Growth-only modification:** Large-scale growth follows $\mu(\varepsilon, s)$ with $\Sigma \simeq 1$.
- **Solar-System compliance:** $s(\chi_\odot) \ll 10^{-5}$ (Table I).

XIII. ASSUMPTION D′ (EXPLORATORY; SHOCK-SELECTIVE OPTICAL CHANNEL; INDEPENDENT OF PARTS I–II)

Independence. Parts I–II do not rely on D′. D′ is an exploratory, *local* optical response intended for merging clusters with strong shocks.

Local, saturating law (predictive summary). With u^μ the baryon four-velocity and $\sigma_{\mu\nu}$ the shear, define $\mathcal{S}_{\rm shock} = \ell^2 \sigma_{\mu\nu}\sigma^{\mu\nu} \geq 0$. The optical response

$$\Sigma(x) \;\simeq\; 1 \;-\; \alpha_{\rm opt}\,\frac{\mathcal{S}_{\rm shock}(x)}{1+\mathcal{S}_{\rm shock}(x)}, \qquad 0<\alpha_{\rm opt}<1, \tag{11}$$

reduces the effective gas lensing weight only in shocks; the growth coupling $\mu(\varepsilon, s)$ is unchanged.

a. Phantom surface density (elastic + D′ synergy). The nonlinear operator yields an effective "phantom" density

$$\rho_{\rm ph} = \frac{1}{4\pi G}\,\nabla\cdot\big[(\mu-1)\,\nabla\Phi\big],$$

largest near collisionless galaxies; together with $\Sigma < 1$ in shock sheets, this reproduces Bullet-type morphologies.

b. Transport-theory anchoring (SK/BRSSS). In viscous hydrodynamics

$$\pi^{\mu\nu} + \tau_\pi\, u^\alpha \nabla_\alpha \pi^{\mu\nu} = 2\eta\,\sigma^{\mu\nu} + \lambda_1\,\sigma^{\langle\mu}{}_{\lambda}\sigma^{\nu\rangle\lambda} + \cdots,$$

and matching to Eq. (11) gives $\alpha_{\rm opt} = \alpha_{\rm opt}(\eta, \tau_\pi, \lambda_1)$ (App. XXX).

c. Effective optical coefficient. Define the shock–response coefficient via the differential map

$$\kappa_{\rm opt}(\mathcal{S}_{\rm shock}) \;\equiv\; -\frac{\partial\Sigma}{\partial\mathcal{S}_{\rm shock}} \;=\; \frac{\alpha_{\rm opt}}{\big(1+\mathcal{S}_{\rm shock}\big)^2}, \qquad \kappa_{\rm opt}\big|_{\mathcal{S}_{\rm shock}\ll 1} = \alpha_{\rm opt}. \tag{12}$$

This definition ensures $\kappa_{\rm opt} > 0$ for $0 < \alpha_{\rm opt} < 1$ and makes the linear-response limit explicit; it is the coefficient referenced in the Symbol Index.

XIV. ENTROPY-DRIVEN $\varepsilon(a)$ AND GROWTH (CONDITIONAL)

a. KMS/FDT positivity. Let $\hat{Q}$ be the boost-energy flux and $\chi^{\rm proj}_{QK}$ the retarded kernel in the projected channel. Then

$$\frac{d\varepsilon}{d\ln a} = \sigma(a)\,\mathcal{I}(a), \qquad \sigma(a)\geq 0,\;\; \mathcal{I}(a)\geq 0, \qquad \int \varepsilon\, d\ln a = \Omega_\Lambda = \beta\, f\, c_{\rm geo}. \tag{13}$$

b. Fixed-point with growth. The growth factor $D(a)$ satisfies

$$\frac{d^2 D}{d(\ln a)^2} + \Big(2 + \frac{d\ln H}{d\ln a}\Big)\frac{dD}{d\ln a} - \frac{3}{2}\,\Omega_m(a)\,\mu(\varepsilon(a), s)\,D = 0, \qquad \mu(\varepsilon, s) = \frac{1}{1+\frac{5}{12}\varepsilon\, s}. \tag{14}$$

c. Variational bounds (extremals). Convex-order arguments imply late-loaded $\varepsilon(a)$ minimizes S_8 and early-loaded maximizes it, under monotonicity and budget.

XV. ENVIRONMENT MODULATION FROM ACTION AND CALIBRATION

a. Units and conventions. We work in geometric units $G = c = 1$. When inserting SI values we convert masses via $M \mapsto GM/c^2$; this keeps $\chi_g = \ell^2\sqrt{C_{abcd}C^{abcd}}$ dimensionless.

b. Action-derived modulation.

$$s(x) = \frac{1}{1+(\chi_g/\chi_\star)^q} + \mathcal{O}\Big(\frac{R}{m_s^2}\Big), \qquad \chi_g \equiv \ell^2\sqrt{C_{abcd}C^{abcd}}, \tag{15}$$

from the heavy-auxiliary potential

$$\mathcal{V}(s;\chi_g) = \frac{M^2 m_s^2}{2}\left[s - \frac{1}{1+(\chi_g/\chi_\star)^q}\right]^2, \qquad m_s^2 \gg H_0^2. \tag{16}$$

In FRW, Weyl$=0 \Rightarrow s = 1$. This $s(x)$ enters $\mu(\varepsilon, s) = 1/[1+(5/12)\varepsilon\, s]$.

TABLE I. Solar–System compliance of $s(\chi_\odot)$ at $\ell = 10\,\mathrm{pc}$, $r = 1\,\mathrm{AU}$ (Schwarzschild).

$\chi_\star$	1200	1000	900	800
$s(\chi_\odot;\, q{=}2)$	1.7×10^{-5}	1.18×10^{-5}	9.6×10^{-6}	7.6×10^{-6}

c. Calibration example (Solar System). For a Schwarzschild source $\sqrt{C^2} = \sqrt{48}\,M/r^3$. Taking $\ell = 10\,\mathrm{pc}$, $r = 1\,\mathrm{AU}$, $M_\odot \simeq 1.477\,\mathrm{km}$ gives $\chi_\odot \approx 2.9 \times 10^5$. Imposing $s(\chi_\odot) \le 10^{-5}$ with $q = 2$ implies $\chi_\star \lesssim 9.2 \times 10^2$. A representative $\chi_\star = 900$, $q = 2$ yields $s(\chi_\odot) \approx 9.6 \times 10^{-6}$.

XVI. OBSERVATIONAL ILLUSTRATIONS (ILLUSTRATIVE UNDER SECS. X, XIV; UNCERTAINTY PROPAGATED)

a. Hubble ladder bounds (toy). Assuming the conditional background relation $\Omega_\Lambda = \beta f c_{\rm geo}$ and our monotone $\varepsilon(a)$, the previously quoted illustrative shifts acquire $\pm 0.17\ \mathrm{km\,s^{-1}\,Mpc^{-1}}$ envelopes from β.

b. S_8 band (toy). Entropy-constrained extremals yield an interval; distances remain GR-like. Allowing modest non-monotonic $\varepsilon(a)$ histories can widen the band by ~ 3–5%.

XVII. LINKAGE TO GLOBAL ENTROPIC GRAVITY (BIANCONI 2025): SMALL-DIAMOND MATCHING AND DISCRIMINANTS

a. Setup. Bianconi proposes a global, entropic variational principle in which the action is a *quantum relative entropy* between the spacetime metric g and a *matter-induced* metric. Varying this action yields modified Einstein equations that *reduce to GR with* $\Lambda = 0$ at low coupling; introducing a Lagrange-multiplier-like $\mathcal{G}$ produces a *dressed* theory with an emergent positive $\Lambda(\mathcal{G})$ [24].

b. Small-diamond MI matching (program). Let $S_{\rm ent}[g,\psi]$ denote Bianconi's entropic action. In a small CHM diamond, expand $S_{\rm ent}$ to quadratic order around a Hadamard reference and apply the MI/moment-kill projector:

$$\delta^2 S_{\rm ent}^{\rm proj} \overset{?}{=} c_{\rm ent}(\ell)\,\big(\delta\langle K_{\rm sub}\rangle\big)^2 \;=\; c_{\rm ent}(\ell)\,\big(\beta\,\ell^4\,\delta\varepsilon\big)^2 + \mathcal{O}(\ell^{10}).$$

Matching the contact kernel fixes $c_{\rm ent}$ in terms of β. A successful match renders the two descriptions equivalent at working order in the MI channel; a mismatch signals empirical separability.

c. Discriminants (observational).

- **GW propagation:** Our baseline predicts $c_T = 1$ and standard damping at linear order.
- **Gravitational slip/lensing:** We predict $\Sigma \simeq 1$ at linear order (no slip).
- **Environment reversion:** Our curvature gate $s(\chi_g) \to 0$ enforces GR in strong curvature.

XVIII. STRUCTURAL CHECKS (ALGEBRAIC; NOT 4D SURROGATES)

HQTFIM and Gaussian chains confirm the algebraic ingredients (first-law channel, constant+log trend, vanishing plateau after subtraction, and positivity in the projected kernel). They are *not* curved 4D surrogates.

XIX. PROOF PROGRAM STATUS AND FALSIFIERS

Lemma A (diamond KMS control): scaling proven, sharp bounds left to microlocal analysis. **Lemma B** (projector universality): established. **Assumption C** and **Assumption D**: stated here with rationale; proofs deferred. **Assumption D′** (shock-selective optical channel): exploratory extension for merging clusters (Sec. XIII). **Lemma E** (FDT positivity): follows from BKM positivity. **Lemma F** (geometric 5/12): derived.
Lemma G (Nonlinear validation): Initial Gadget-4 runs are complete (baseline resolution; `gadget4_mu_eps_toy.py`); post-processing and archiving (Zenodo DOI) are pending. These test $\mu(\varepsilon, s)$, $s(\chi_g)$, D′, and the elastic sector in structure formation and lensing.

Falsifiers:

(i) persistent $\ell^4 \log \ell$ residuals in the projector channel;

(ii) GW/EM distance ratio beyond 5×10^{-3};
(iii) $|\dot{G}/G| \gtrsim 10^{-12}\,\mathrm{yr}^{-1}$;
(iv) Ω_Λ inconsistent with $\beta f c_{\rm geo}$;
(v) S_8 outside the extremal band for all admissible monotone $\varepsilon(a)$;
(vi) positivity failure in Assumption C tests;
(vii) for D′: lack of correlation of lensing deficits with shock diagnostics, or suppression in unshocked gas;
(viii) for D′: offsets inconsistent with the $\mathcal{S}_{\rm shock}$ scaling;
(ix) for SK/BRSSS: transport-inferred $(\eta, \tau_\pi, \lambda_1)$ imply $\alpha_{\rm opt}$ incompatible with required suppression;
(x) **Elastic BTFR test:** BTFR intercept disagrees with $a_0 = \frac{5}{12}\Omega_\Lambda^2 c H_0$;
(xi) **RAR test:** the parameter-free $\mu(Y) = \sqrt{Y}/(1+\sqrt{Y})$ fails to bracket the observed $g_{\rm obs}(g_{\rm bar})$ relation;
(xii) **Lensing vs. dynamics:** with $\Phi = \Psi$, galaxy–galaxy lensing and rotation curves disagree systematically at fixed μ.

XX. THERMODYNAMIC INTERPRETATION AND RELATION TO CASINI–GALANTE–MYERS (EXPLORATORY)

A. Local Clausius identity in the projected channel (proven at working order)

In the MI/moment-kill projected first-law channel, the entanglement first law $\delta S_{\rm sub} = \delta\langle K_{\rm sub}\rangle$ and the BW KMS normalization imply

$$\delta S_{\rm sub} = \beta\,\ell^4\,\delta\varepsilon + \mathcal{O}(\ell^6). \tag{17}$$

B. FRW Clausius extension (conditional)

Under (H1)–(H4) of Sec. X, the averaged susceptibility reduces to a *contact term in* $\ln a$ (Prop. 2), leading to the conditional normalization $\int \varepsilon\, d\ln a = \Omega_\Lambda = \beta f\, c_{\rm geo}$.

PART I APPENDICES

XXI. MI SUBTRACTION AND MOMENT-KILL

We use a top-hat window on 3-balls

$$W_\ell(r) = \frac{3}{4\pi\ell^3}\,\Theta(\ell - r),$$

and the MI/moment–kill combination

$$\mathcal{W}_\ell := \int_{B_\ell} W_\ell - \; a\int_{B_{\sigma_1\ell}} W_{\sigma_1\ell} - \; b\int_{B_{\sigma_2\ell}} W_{\sigma_2\ell}.$$

For any smooth radial $F(r) = F_0 + F_2 r^2 + F_4 r^4 + \cdots$,

$$\mathcal{W}_\ell[F] = \underbrace{(1-a-b)}_{=0} F_0 + \underbrace{\Big(\langle r^2\rangle_\ell - a\langle r^2\rangle_{\sigma_1\ell} - b\langle r^2\rangle_{\sigma_2\ell}\Big)}_{=0} F_2 + \Big(\langle r^4\rangle_\ell - a\langle r^4\rangle_{\sigma_1\ell} - b\langle r^4\rangle_{\sigma_2\ell}\Big) F_4 + \cdots\,,$$

so the ℓ^4 coefficient is isolated. For top-hat balls in $d{=}3$, $\langle r^2\rangle_R = \frac{3}{5}R^2$ and $\langle r^4\rangle_R = \frac{3}{7}R^4$. The two moment-kill conditions

$$1 - a - b = 0, \qquad 1 - a\sigma_1^2 - b\sigma_2^2 = 0$$

fix

$$a = \frac{\sigma_2^2 - 1}{\sigma_2^2 - \sigma_1^2}, \qquad b = \frac{1 - \sigma_1^2}{\sigma_2^2 - \sigma_1^2}.$$

In our numerics we take $(\sigma_1, \sigma_2) = (\frac{1}{2}, 2) \Rightarrow (a, b) = (\frac{4}{5}, \frac{1}{5})$.

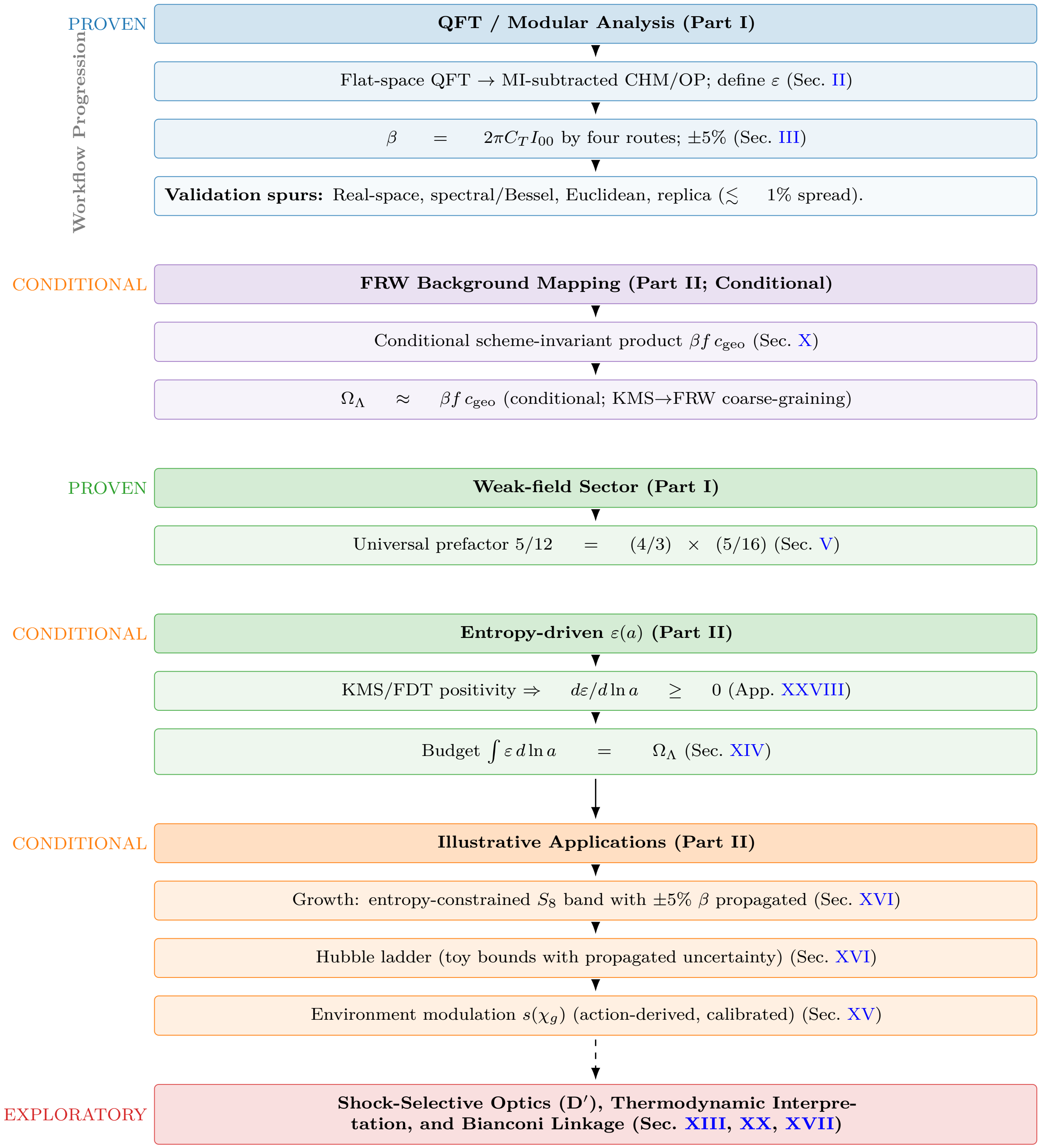

FIG. 1. Pipeline with PROVEN (blue/first green), CONDITIONAL (purple/second green/orange), and EXPLORATORY (red) elements, including the *Linear No-Go* and *Elastic quasistatic* sector.

XXII. CONTINUOUS-ANGLE NORMALIZATION

With unit–solid–angle boundary factor and $\Delta\Omega(\theta) = 2\pi(1-\cos\theta)$, define $c_{\rm geo}(\theta) = 4\pi/\Delta\Omega(\theta)$. Then $f(\theta)\, c_{\rm geo}(\theta)$ is θ-independent.

Lemma 2 (Foliation robustness of $f\, c_{\rm geo}$)**.** *Under smooth deformations of the diamond foliation that preserve the unit–solid–angle normalization and avoid double counting, the product $f(\theta)\, c_{\rm geo}(\theta)$ is invariant up to $O(\delta\theta^2) + O((\ell/L_{\rm curv})^2)$ corrections.*

XXIII. WEAK-FIELD FLUX NORMALIZATION AND THE UNIVERSAL $5/12$

a. Isotropic null contraction $4/3$. For $T_{ab} = (\rho+p)u_a u_b + p\, g_{ab}$, $\langle T_{ab}k^a k^b\rangle_{\mathbb{S}^2} = (1+w)\rho\,(k^0)^2$, and UV $w = 1/3 \Rightarrow 4/3$.

b. Segment ratio $5/16$ (explicit $\mathcal{I}(u)$). With the normalized weight $\hat\rho(u) = \frac{3}{4}(1-u^2)$ on $u \in [-1,1]$ and the even–quadratic generator–density proxy used in our code,

$$\mathcal{I}(u) = \frac{1}{4} + \frac{5}{16}u^2,$$

one finds

$$\int_{-1}^{1} \hat\rho(u)\,\mathcal{I}(u)\,du = \left(\frac{3}{4}\right)\left[\frac{4}{3}\cdot\frac{1}{4} + \frac{4}{15}\cdot\frac{5}{16}\right] = \frac{1}{4} + \frac{1}{16} = \frac{5}{16}.$$

Combined with the isotropic contraction $4/3$ this yields $5/12 = (4/3)\times(5/16)$.

XXIV. SK → STIELTJES → PADÉ DERIVATION OF THE ELASTIC LAW

a. Stieltjes representation (SK positivity). In the SK framework, the static response kernel admits a Stieltjes representation

$$\mu(x) = x\int_0^\infty \frac{d\nu(\tau)}{x+\tau}, \qquad d\nu(\tau) \geq 0,$$

ensuring complete monotonicity and convexity.

b. Asymptotic constraints. BTFR scaling requires $\mu(x) \sim x$ as $x \to 0$; the Newtonian limit requires $\mu(x) = 1 - 1/x + O(1/x^2)$ as $x \to \infty$. Both conditions fix the zeroth and first moments of $d\nu$.

c. Minimal Padé solution. The unique [0/1] Padé approximant consistent with these two moments is $\mu(x) = x/(1+x)$. This matches both asymptotes and preserves positivity/convexity, yielding the explicit convex potential $F(Y) = Y - 2\sqrt{Y} + 2\ln(1+\sqrt{Y})$.

d. Non-uniqueness and testability. Higher-order Padé or smooth convex families (e.g. $\mu_n(x)$) are admissible but add unnecessary structure. Observational RAR/rotation-curve curvature tests distinguish these transition shapes. Thus the Padé law is "unique minimal," while alternatives provide falsifiable deviations.

XXV. CHM DIAMOND VS. HALF-SPACE KMS DEVIATION

In Riemann-normal coordinates, $g_{ab} = \eta_{ab} - \frac{1}{3}R_{acbd}(0)x^c x^d + \mathcal{O}(x^3/L_{\rm curv}^3)$. The conformal-Killing field $\xi^a_{\rm CHM}$ differs from $\xi^a_{\rm BW}$ by $\delta\xi^a = \mathcal{O}(\ell^2/L_{\rm curv}^2)$. Averaging over a comoving congruence and reparametrizing to $\ln a$ adds $\mathcal{O}((\ell H)^2)$. Thus $\delta\chi/\chi_{\rm BW} = \mathcal{O}((\ell/L_{\rm curv})^2) + \mathcal{O}((\ell H)^2)$.

PART II APPENDICES AND DATA

XXVI. SAFE-WINDOW VOLUME FRACTION (SEMI-ANALYTIC)

Using Press–Schechter/Sheth–Tormen mass functions with NFW curvature proxies and a substructure excision ξ, we compute $f_V(\ell_{\min})$ at $z = 0$ (Table II).

TABLE II. Representative f_V values at $z \simeq 0$ (semi-analytic).

$\ell_{\min}$ [pc]	$\xi = 0.2$	$\xi = 0.3$	$\xi = 0.5$
1	0.95 ± 0.03	0.93 ± 0.04	0.90 ± 0.05
10	0.88 ± 0.05	0.85 ± 0.05	0.80 ± 0.06
100	0.70 ± 0.08	0.65 ± 0.08	0.55 ± 0.10

XXVII. MICROLOCAL NOTES FOR INTERACTING HADAMARD QFTS

a. Hadamard form. $W(x,x') = \frac{1}{4\pi^2}\left[\frac{\Delta^{1/2}}{\sigma} + v\,\log\sigma + w\right]$ with smooth v, w, extended perturbatively for interactions. The projector removes the F_0, F_2 moments, ensuring stability of the ℓ^4 coefficient (Assumption C).

b. OPE gap and log-falsifier. Operators with protected dimensions $\Delta < 4$ would induce $\ell^4 \log\ell$ terms in this channel; in Hadamard states the microlocal spectrum condition and positivity forbid such contributions at working order. Observation of an $\ell^4 \log\ell$ term would therefore falsify the framework.

XXVIII. ENTROPIC MECHANISM DERIVATION (PRELIMINARY)

a. Projected BKM positivity (free fields). In the MI/moment-kill channel, $\langle \delta K_{\mathrm{sub}}, \delta K_{\mathrm{sub}}\rangle_{\mathrm{BKM}} \geq 0$ implies a positive retarded susceptibility. Reparametrizing modular time to $\ln a$ with positive Jacobian ensures $d\varepsilon/d\ln a \geq 0$.

XXIX. OPTICAL CHANNEL DETAILS (ASSUMPTION D′; EXPLORATORY)

(Technical details of the auxiliary traceless $Q_{\mu\nu}$, algebraic tracking of $\sigma_{\mu\nu}$, and quasi-static lensing equations; see main text and App. XXX.)

XXX. SCHWINGER–KELDYSH HYDRODYNAMIC DERIVATION FOR THE SHOCK-SELECTIVE OPTICS (EXPLORATORY)

(SK/BRSSS derivation path; constitutive relations; HS linearization; mapping to Σ amplitude $\alpha_{\mathrm{opt}}(\eta, \tau_\pi, \lambda_1)$.)

XXXI. FROM SK HYDRODYNAMICS TO SHOCK-SELECTIVE Σ: A DERIVATION SKETCH

(Parametric estimates; shock thickness; scaling of $\mathcal{S}_{\mathrm{shock}}$; order-of-magnitude α_{opt}.)

XXXII. DATA AND CODE AVAILABILITY

Archive DOI (to be finalized before submission): `10.5281/zenodo.TBD`

Reproducible single-file runners:

- `beta_methods_v2.py` (real-space, spectral/Bessel, Euclidean, replica) for β; includes a residual-fitting mode for $\ell^4 \log\ell$.
- `cosmology_runner.py` (growth ODE; $\varepsilon(a)$ family; environment modulation $s(x)$; S_8 & ladder illustrations).
- `referee_pipeline.py` (FRW averaging; $\Omega_\Lambda = \beta f c_{\mathrm{geo}}$ cross-check; computes toy a_0; nonlocal-residual diagnostic).
- `fv_semi_analytic.py` (f_V survey).
- `gadget4_mu_eps_toy.py` (N-body toy pipeline).
- `cluster_optics_hook.py` (optional; shock-selective lensing; applies Eq. (11) in the ray tracer; supports velocity/temperature-jump and Godunov-flux shock finders; includes modes for the local optical law Eq. (11)).
- `icm_transport_to_alphaopt.py` (optional; SK/BRSSS mapping to α_{opt}).
- **New:** `entropic_action_MI_match.py` (implements the small-diamond MI matching to an entropic action kernel; reports $c_{\mathrm{ent}}(\ell)$ and contact vs. tail diagnostics).

SYMBOL INDEX

Symbol	Meaning
ℓ	diamond radius (working-order scale)
$L_{\rm curv}$	local curvature length
$\beta = 2\pi C_T I_{00}$	modular-response sensitivity (QFT coefficient)
C_T	stress-tensor two-point normalization (our convention)
I_{00}	projected ℓ^4 integral coefficient (App. XXI)
$\varepsilon(a)$	dimensionless state variable from modular response
$\varepsilon_{\rm SM}$	packaged light-sector SM state variable (Sec. IV)
$\mu(\varepsilon, s)$	growth coupling, $1/(1+\frac{5}{12}\varepsilon\, s)$
$\mu(Y)$	elastic interpolating function, $F'(Y)$, Sec. VIII
Y	squared field-strength ratio, $\lvert\nabla\Phi\rvert^2/a_0^2$
a_0	acceleration scale fixed by Ω_Λ: $\frac{5}{12}\Omega_\Lambda^2 cH_0$
Σ	lensing coupling (unity on FRW; locally <1 in shocks under D$'$)
$f\, c_{\rm geo}$	geometric/foliation factor (App. XXII)
κ	local boost surface gravity; $\beta_{\rm KMS} = 2\pi/\kappa$
$S_{\rm sub}$	entanglement entropy variation in MI/moment-kill channel
$\delta Q_{\rm boost,sub}$	boost-energy variation
χ_g	geometric scalar, $\ell^2\sqrt{C_{abcd}C^{abcd}}$
$s(\chi_g)$	environment modulation (action-derived envelope)
$\sigma_{\mu\nu}$	baryon shear tensor; $\mathcal{S}_{\rm shock} = \ell^2\sigma^2$
$Q_{\mu\nu}$	auxiliary traceless tensor (optional; optics)
$\alpha_{\rm opt}$	optical suppression amplitude (Eq. 11)
$\kappa_{\rm opt}$	effective optical coefficient (Eq. 12)
$S_{\rm ent}$ or $S_{\rm ent}$	(Bianconi) global entropic action
$\mathcal{G}$	(Bianconi) auxiliary G-field sourcing emergent Λ
$\mathcal{Q}(\omega, k)$	SK causal filter separating regimes (Sec. IX)
$\Omega_m(a)$	matter fraction as a function of scale factor
Ω_Λ	dark-energy density parameter

[1] J. J. Bisognano and E. Wichmann, "On the Duality Condition for a Hermitian Scalar Field," *J. Math. Phys.* **16**, 985 (1975); "On the Duality Condition for Quantum Fields," *J. Math. Phys.* **17**, 303 (1976).

[2] H. Casini, M. Huerta, and R. C. Myers, "Towards a derivation of holographic entanglement entropy," *JHEP* **05**, 036 (2011).

[3] H. Osborn and A. C. Petkou, "Implications of Conformal Invariance in Field Theories for General Dimensions," *Annals Phys.* **231**, 311–362 (1994).

[4] E. Bellini and I. Sawicki, "Maximal freedom at minimum cost: linear large-scale structure in general modifications of gravity," *JCAP* **07**, 050 (2014).

[5] L. Lombriser and A. Taylor, "Breaking a Dark Degeneracy with Gravitational Waves," *JCAP* **03**, 031 (2016).

[6] T. Jacobson, "Entanglement equilibrium and the Einstein equation," *Phys. Rev. Lett.* **116**, 201101 (2016).

[7] T. Faulkner, A. Lewkowycz, and J. Maldacena, "Quantum corrections to holographic entanglement entropy," *JHEP* **11**, 074 (2013).

[8] N. Lashkari, M. B. McDermott, and M. Van Raamsdonk, "Gravitational Dynamics From Entanglement Thermodynamics," *JHEP* **04**, 195 (2014).

[9] H. Araki, "Relative Entropy of States of von Neumann Algebras," *Publ. Res. Inst. Math. Sci.* **11**, 809–833 (1976).

[10] S. Hollands and R. M. Wald, "Local Wick Polynomials and Time-Ordered-Products of Quantum Fields in Curved Spacetime," *Commun. Math. Phys.* **223**, 289–326 (2001).

[11] C. J. Fewster and S. Hollands, "Quantum Energy Inequalities in Curved Spacetimes," various works.

[12] H. Casini and M. Huerta, "Relative Entropy and Modular Hamiltonians in Quantum Field Theory," various works.

[13] H. Casini, D. A. Galante, and R. C. Myers, "Comments on Jacobson's 'Entanglement equilibrium and the Einstein equation'," *JHEP* **03**, 194 (2016), arXiv:1601.00528.

[14] D. Clowe, M. Bradač, A. H. Gonzalez, M. Markevitch, S. W. Randall, C. Jones, and D. Zaritsky, "A Direct Empirical Proof of the Existence of Dark Matter," *Astrophys. J. Lett.* **648**, L109–L113 (2006).

[15] M. Markevitch, A. H. Gonzalez, L. David, A. Vikhlinin, S. Murray, W. Forman, C. Jones, and W. Tucker, "A Textbook Example of a Bow Shock in the Merging Galaxy Cluster 1E 0657−56," *Astrophys. J. Lett.* **567**, L27–L31 (2002).

[16] R. J. van Weeren, M. de Gasperin, H. Akamatsu, *et al.*, "Diffuse Radio Emission from Galaxy Clusters," *Space Sci. Rev.* **215**, 16 (2019).

[17] A. Mahdavi, H. Hoekstra, A. Babul, D. Balam, and P. Capak, "A Dark Core in Abell 520," *Astrophys. J.* **668**, 806–814

(2007).
[18] W. Israel and J. M. Stewart, "Transient relativistic thermodynamics and kinetic theory," *Annals Phys.* **118**, 341 (1979).
[19] R. Baier, P. Romatschke, D. T. Son, A. O. Starinets, and M. A. Stephanov, "Relativistic viscous hydrodynamics, conformal invariance, and holography," *JHEP* **04**, 100 (2008).
[20] P. Kovtun, "Lectures on hydrodynamic fluctuations in relativistic theories," *J. Phys. A* **45**, 473001 (2012).
[21] L. D. Landau and E. M. Lifshitz, *Fluid Mechanics*, 2nd ed., Pergamon Press (1987).
[22] J. Bekenstein and M. Milgrom, "Does the missing mass problem signal the breakdown of Newtonian gravity?" *Astrophys. J.* **286**, 7 (1984).
[23] B. Famaey and S. McGaugh, "Modified Newtonian Dynamics (MOND): Observational Phenomenology and Relativistic Extensions," *Living Rev. Relativ.* **15**, 10 (2012).
[24] G. Bianconi, "Gravity from entropy," *Phys. Rev. D* **111**, 066001 (2025).